THE JOURNAL OF PHYSICAL CHEMISTRY B

ARTICLE

pubs.acs.org/JPCB

DFT Study of the Interaction between Alkaline Cations and Molecular Bowls Derived from Fullerene

Jorge A. Carrazana-García,[†] Jesús Rodríguez-Otero,[‡] and Enrique M. Cabaleiro-Lago[†,*]

[†]Departamento de Química Física, Facultade de Química, Universidade de Santiago de Compostela. Campus de Lugo. Avda. Alfonso X El Sabio s/n 27002 Lugo (Spain)

[‡]Departamento de Química Física, Facultade de Ciencias, Universidade de Santiago de Compostela. Avda. das Ciencias s/n, 15782 Santiago de Compostela (Spain)

Supporting Information

ABSTRACT: A systematic study of the interaction of alkaline cations with curved π systems (molecular bowls) derived from fullerene (C_{60}) shows the ability of these structures to form stable cation$-\pi$ complexes with both of their sides: concave and convex. In all cases, complexes with the cation in the convex side are more stable than its corresponding partner inside the bowl. When forming the complexes with the alkaline cations, these bowls exhibit great stability but several descriptors that usually work in planar conjugate molecules (like the magnitude of the charge transferred to the cation or the cation$-$ligand distance) do not properly describe the trends observed. The present study shows that with these curved π systems inductive effects play a central role in the formation of complexes with alkaline cations. This conclusion contradicts the simplistic point of view on the dominant effect of the electrostatic term in the interaction between alkaline cations and bowls derived from fullerene. Additionally, steric effects can be relevant when bulky cations are placed in the concave side of the largest bowls.

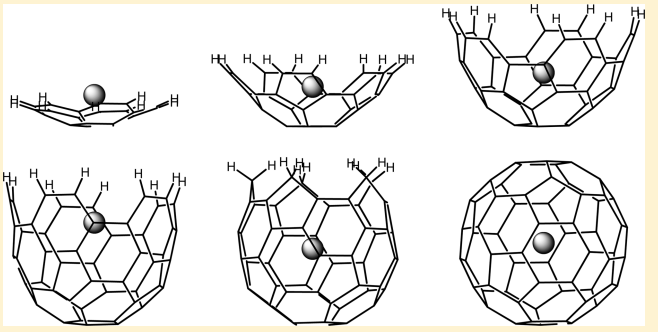

INTRODUCTION

Cation$-\pi$ complexes of aromatic compounds have received great attention in recent years, in part as a result of the role they are believed to play in protein folding, neurological signaling, the functioning of certain ion channels, and other diverse biological phenomena.[1] From these studies, there has emerged a general consensus that the degree to which cations are attracted to the electron-rich π clouds correlates with the electrostatic potentials of the π systems.[2]

When the π system is curved, other aspects increase their importance in the description of the interaction, mainly as a consequence of the asymmetry in the electrostatic potential of these species, regarding their concave and convex sides, but also due to the presence of significant inductive effects in some of these systems. Additionally, as the curvature increases, the steric repulsion becomes significant for the interaction between the concave side of the curved π systems and bulky cations.

Curved π systems constituted as fragments of fullerenes exhibit multisite coordination possibilities. The study of relative preferences of the convex and concave faces of these bowls for binding metal centers, especially involving transition-metal atoms, has been a focus of considerable interest in the recent years due to its fundamental and practical importance.[3]

In the present work, a systematic study of complexes formed by alkaline cations and a series of curved π systems (molecular bowls "MB") derived from buckminsterfullerene was carried out to shed light on these interactions. The MB series was designed as C_{60} fragments saturating the outer rim of carbon atoms with H atoms. The series begins with corannulene $C_{20}H_{10}$ (labeled as P1) adding pentagonal or hexagonal rings (faces) to complete the buckminsterfullerene structure, as shown in Chart 1. In the sequence P1$-$P2$-$P3$-$P4, a constant increment of 10 carbon atoms is added to the previous member but, in the last two increments, P4$-$P5 and P5$-C_{60}$, only 5 carbons atoms are incorporated. In this series, P5 is the only structure with saturated carbon atoms and fullerene the only one without hydrogen atoms. The complex formation ability of these MBs was explored locating the cations in different positions: above the bonds, above the pentagonal and hexagonal rings, and exploring the concave and convex sides of the π surface.

Computational Details. All of the calculations were carried out with the *Gaussian03* suite of programs,[4] employing the B3LYP method.[5] The 6-31+G* basis set was used for all MB's and for Li^+, Na^+, and K^+ cations. For Rb^+ and Cs^+, the effective core potential LANL2DZ basis set (Los Alamos National Laboratory 2 double ζ) was employed.[6] This combination of a

Received: October 8, 2010
Revised: January 12, 2011
Published: March 08, 2011

Chart 1. Structures of C_{60} and the Molecular Bowls Studied

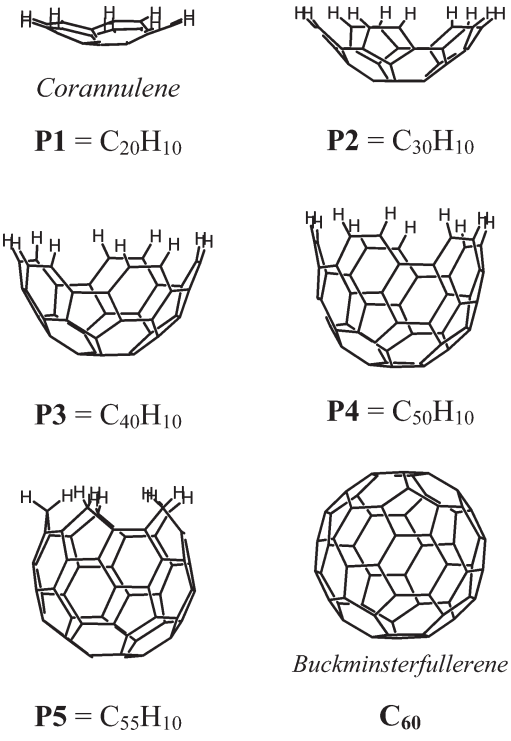

hybrid DFT method with a split valence plus polarization basis set has proven[7] to be a good choice for obtaining reliable results with low-to-moderate computational cost in similar systems.

Different possible structures with the cations located on the hexagonal faces as well as on pentagonal faces of all of the MBs were considered. The corresponding complexes were fully optimized (no symmetry restrictions) starting from structures with the cation centered on the different faces of both sides, concave (inner) and convex (outer), of the MB. Several structures with the cations over the edges of pentagons and hexagons were additionally explored. Frequency calculations were carried out for the smallest members of the series to verify that the optimized geometries correspond to minima of the bowl−cation potential energy surface. In complexes with larger bowls, frequency calculations were limited by the computational resources available. However, it was assumed that the stationary points that have been found correspond to minima based on the results obtained for similar structures with the smallest bowls.

Complexation energies were obtained by using the counterpoise method of Boys and Bernardi[8] to correct for the basis set superposition error. Thus, the interaction energy is obtained by subtracting from the complex energy the energies of the fragments (bowl and cation) employing the geometry and the whole basis set of the complex. As the geometry of the bowl changes when the complex is formed, an additional contribution describing this effect must be included. This deformation energy is obtained as the energy difference between the bowl in the complex geometry and in isolation.[8]

RESULTS AND DISCUSSION

Molecular Bowls. The structures of the MBs are shown in Chart 1, whereas selected parameters of the optimized geometries

Table 1. Selected Geometric Parameters of Buckminsterfullerene and the Molecular Bowls Optimized at the B3LYP/6-31+G* Level: Bond Length (r), Plane Angles (A1, A2), Dihedral Angles (D1, D2), and POAV Values at C1, C2, and C3, as Defined in the Drawings below

	P1	P2	P3	P4	P5	C_{60}
r (Å)	1.418	1.436	1.452	1.454	1.453	1.454
A1 (°)	108.0	108.0	108.0	108.0	108.0	108.0
D1 (°)	153.2	140.4	141.1	141.3	142.4	119.9
A2 (°)	123.9	119.2	119.2	119.5	119.9	120.0
D2 (°)	158.9	142.3	137.9	136.8	137.8	138.1
POAV						
C1 (°)	8.1	12.4	12.1	12.1	11.7	11.6
C2 (°)	3.7	8.6	11.1	11.9	11.8	11.6
C3 (°)	1.6	7.0	10.4	11.6	11.7	11.6

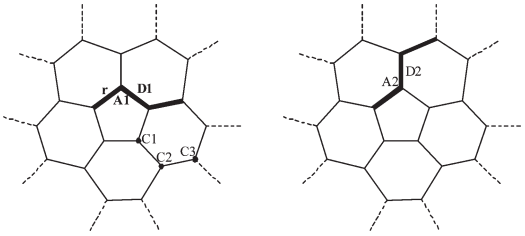

are listed in Table 1. All of these structures show a remarkable stiffness and the geometric parameters (bond distances, plane and dihedral angles) of the structures remain similar as the MB grows. The only faces that exhibit certain differences in their geometries are the ones closer to the rim. In the pentagonal bottom end, the geometrical differences become smaller once the next first or second ring of faces are added: P1H1 faces are slightly bigger and joined to the bottom by a wider dihedral angle than P2H1 faces, but the differences are smaller between P2H1 and P3H1 and so on. In fact, P3H1 faces show no major differences with those of the larger members of the series, P4H1 and P5H1, and C_{60}. [The labels of the lateral faces are constructed using the following system: the first characters design the bowl (P1 to P5 or C_{60}), the next character is "H" for hexagonal faces or "P" for pentagonal ones and the last character groups equivalent faces by its distance to the bottom (explanatory schemes in Figure 4)].

The π-orbital axis vector (POAV) method proposed by Haddon[9] has often been applied to describe curved surfaces.[10] The π-orbital axis vector is defined as that vector, which makes equal angles ($\theta_{\sigma\pi}$) to the three σ-bonds at a conjugated carbon atom, and the pyramidalization angle is obtained as $\theta_P = (\theta_{\sigma\pi} - 90)$. The pyramidalization angle is a useful quantity to gauge the deviation from the planarity of the carbon atoms in the nonplanar conjugated organic molecules, for example bridged annulenes and fullerenes. As reported before in a study about bowl−nanotube transition,[11] bowl-like structures exhibit a variable degree of pyramidalization at carbon atoms depending on their position. Because of the C5v symmetry of this MB series, concentric rings of carbons with equivalent POAV angles can be defined. The progression of POAV angle value from the bottom ring (ring 1) to the rim-ring (ring n) is a characteristic of the bowl topography. In P1, the pyramidality of the carbon atoms

dx.doi.org/10.1021/jp109654e |J. Phys. Chem. B 2011, 115, 2774–2782

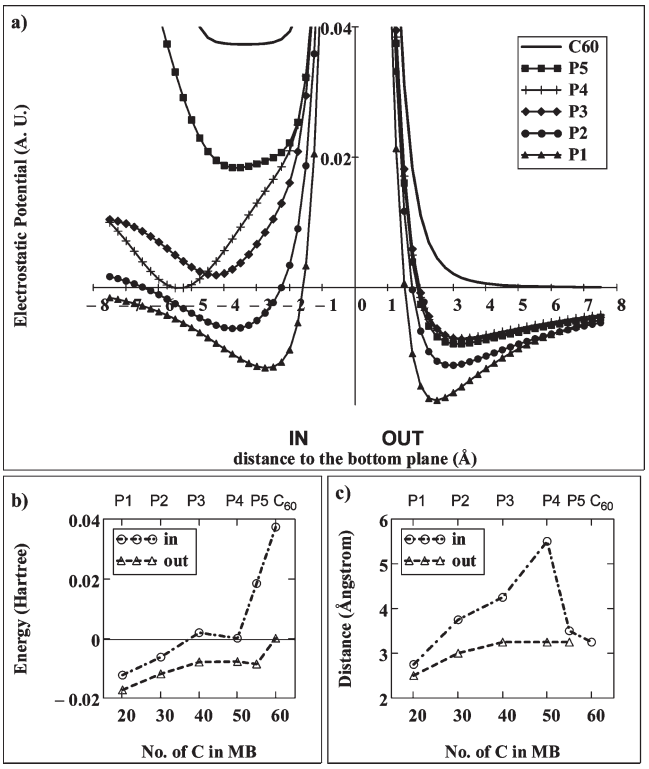

Figure 1. a) Electrostatic potential along the C5 axis of C_{60} and the molecular bowls studied. The zero distance value corresponds to the plane of the central pentagon (the "bottom" of the MBs or one pentagonal face of fullerene); negative distances correspond to the inner (concave) part and positive ones to the outer (convex) part of the curved surfaces. Plots **b**) and **c**) summarize the properties of the minima in the electrostatic potential of the bowls.

in the pentagon is 8.1°, but already in P2 these carbons are essentially as pyramidal (POAV = 12.4°) as those in C_{60} (POAV = 11.6°). Analyzing the complete sequence P1...P5, C_{60}, a pattern of almost constant curvature appears for the lower ring numbers and only slight deviations are observed in the n and $(n-1)$ rings. Other parameters were explored as a measure of the growing pattern of the MBs (such as the angle between the vectors normal to the bottom and to the rim faces, the area of the vertical symmetry plane inscribed by each MB, or the distance from the bottom center to the MB centroid) but they do not provide any new features.

The molecular electrostatic potential (MEP) calculated along the C5 axis of the bowls is showed in part a of Figure 1 as a function of the distance to the bottom pentagonal ring. As reported previously,[12−14] the results show that the curvature of these systems generates important differences between the concave and convex sides. In part b of Figure 1, it can be seen that MEP values along this axis always have more negative minima in their outer (convex) side than in the inner (concave) side, even when there could be other regions with different behaviors.

Focusing the attention in the minima along the C5 axis, we can observe that the MEP at the minimum increases with the MB size (part b of Figure 1) with one exception in each series (P4 in the inner and P5 in the outer) that breaks the main tendencies. All of the MEP profiles along the C5 axis of the bowls exhibit minima with negative values in their convex side, whereas the same is true only for the inner side of the smallest bowls (P1 and P2). These

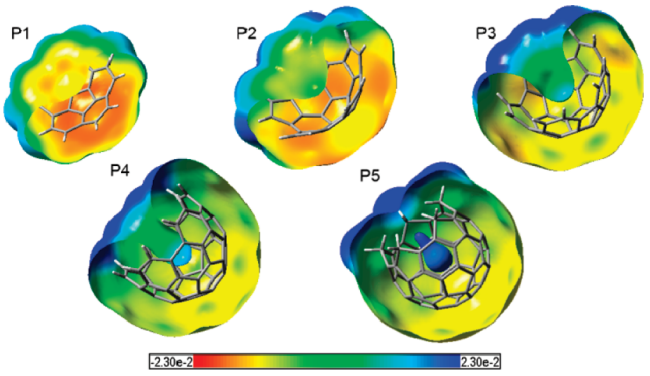

Figure 2. Molecular electrostatic potential maps of the bowls obtained at the B3LYP/6-31+G* level for the P1−P5 molecular bowls. Electrostatic potentials are mapped onto an electron density isosurface of 0.0002 au. The red surface corresponds to a negative region of the electrostatic potential (−0.023 au), whereas the blue color corresponds to regions where the potential is positive (+0.023 au).

minima are located (part c of Figure 1) at longer distances as the MB grows reaching a constant value for P3, P4, P5 in the convex part, whereas the minima move to shorter distances in the sequence P4, P5, C_{60} in the inner side. The MEP values shown by the concave side of P4 differ markedly with respect to the rest of the members of the series. This structure has already aroused interest because it could represent a sort of transition between bowls and nanotubes.[11]

A more complete view of the MEP of the MBs is shown in Figure 2. In all cases, the outer sides present more negative MEP values than the corresponding inner positions. The concave side changes regularly from slightly negative to markedly positive MEP values in the P1-to-P5 sequence. It is worth noting that in P3 and especially in P4 the deepest region of the cavity is more positive than the region near the rim of these bowls. This is decisive for understanding the equilibrium position adopted by the least polarizing cations (K^+, Rb^+, and Cs^+) in their inner complexes with P4. The almost closed cavity of P5 with high positive MEP values implies that this is a repulsive site for cations. Nevertheless, as shown below, the total interaction energy reaches significant negative values in the inner complexes between P5 and the smallest alkaline cations, indicating that the electrostatic interaction is not always the most important one in these systems. In fact, the polarizabilities of the bowl series increase systematically with MB size (34.8, 54.0, 65.9, 77.2, 79.3, and 81.0 $Å^3$, from P1 to C_{60}, at the level of calculation described above) suggesting a major role of inductive effects in complexes formed with larger bowls.

Complexes (MB/Cation). At the level of calculation used in this work, alkaline cations form stable complexes with all the studied bowls on both sides, convex and concave. There are stationary points located in all hexagonal and pentagonal faces explored. The only exceptions are the pentagons closer to the rim of P5, which are the only rings with saturated carbon atoms; during optimization, the cations originally on this face move to one of the adjacent hexagonal faces. In the outer part of the bowls, all other positions are accessible and well differentiated geometrically, whereas, in the inner side, because of curvature and steric impediment, there are a limited number of positions available to the cations (Table 2). The outer complexes are always more stable than their inner counterparts. These results are in agreement with previous calculations on

dx.doi.org/10.1021/jp109654e |J. Phys. Chem. B 2011, 115, 2774–2782

Table 2. Counterpoise Corrected Complexation Energies (in kcal/mol) for Complex Formation between Molecular Bowls (MB) and Alkaline Cations Obtained with the B3LYP Method and 6-31+G* (for C, H, Li, Na, and K) or LANL2DZ (for Rb and Cs) Basis Set[a]

MB/Cation	Li^+ in	Li^+ out	Na^+ in	Na^+ out	K^+ in	K^+ out	Rb^+ in	Rb^+ out	Cs^+ in	Cs^+ out
P1 = $C_{20}H_{10}$										
Bottom	−39.58	−43.46	−27.01	−30.07	−19.87	−21.25	−16.20	−17.49	−13.69	−15.02
P1H1	−41.30	−43.77	−27.32	−30.04		−20.69		−16.90		−14.36
P2 = $C_{30}H_{10}$										
Bottom	−38.61	−40.12	−26.96	−28.83	−19.37	−20.19	−15.77	−16.87	−13.10	−14.45
P2H1	−39.06	−44.11	−26.90	−31.18		−21.77		−17.96		−15.32
P2P1		−46.30		−31.20		−21.41		−17.39		−14.69
P3 = $C_{40}H_{10}$										
Bottom	−32.76	−39.18	−21.78	−27.32	−15.98	−19.05	−12.64	−15.75	−9.151	−13.42
P3H1	−33.91	−40.26	−23.44	−28.57		−19.91		−16.47		−14.04
P3P1		−42.08		−29.04						
P3H2	−37.83	−44.36		−30.24		−20.45		−16.52		−13.84
P4 = $C_{50}H_{10}$										
Bottom	−31.77	−40.83	−20.17	−28.56	−18.79	−19.72	−14.40	−16.34	−7.45	−13.90
P4H1	−32.53	−40.36	−20.27	−28.65		−19.87		−16.40		−13.93
P4P1		−40.88		−28.22						
P4H2	−34.03	−40.63	−26.02	−28.15		−19.04		−15.45		−12.92
P4H3	−38.02	−42.27		−28.23		−18.66		−14.88		−12.34
P5 = $C_{55}H_{10}$										
Bottom	−31.75	−41.96	−18.62	−29.56	−10.40	−20.57	−3.36	−17.12	+10.11	−14.63
P5H1	−31.92	−41.61	−18.74	−29.70		−20.74		−17.19		−14.66
P5P1		−41.59		−28.86						
P5H2	−32.20	−40.18	−18.87	−28.13		−19.11		−15.55		−13.02
P5H3	−32.59	−40.00		−26.83		−17.48		−13.90		−11.49
C_{60} P face	−20.44	−32.97	−7.04	−21.50	+0.58	−13.52	+8.26	−10.45	+21.98	−8.35

[a] The labeling of the lateral faces is shown in Figure 4.

complexes between cations and curved π systems[12] as well as with some experimental results.[13] The reverse situation, i.e. the preferential binding of cations to the concave side of MBs, or bowls with more negative MEP inside has also been reported.[14] Nevertheless, the level of calculation used in these works (AM1 in ref 14a AM1, HF/6-31G* and pBP/DN** in ref 14b, and B3LYP/3-21G in ref 14c) seems not to be enough for properly describing the properties of MBs and their interaction with cations.

Structures with the alkaline cation located over the C−C bonds of P1 are transition states for the migration of the cation from one ring to another, as confirmed by the presence of one imaginary frequency corresponding to cation displacement between rings. Figure 3 shows the barrier heights calculated for the system P1/Li^+. The values of the barriers for the face-to-face migration in the inner side of P1 are small and similar to the reported barriers for the endohedral C_{60}/Li^+ complexes.[15] A similar behavior can be expected for the other bowls studied (P2 to P5). The barriers in the concave side are small, so it is reasonable to consider that close to room temperature even small cations as Li^+ that energetically distinguish among faces will actually be dynamically migrating from one face to another (trajectory calculations[15] in Li^+@C_{60} support this conclusion). In the case of complexes with the outer side of the bowl, the barriers are higher and the faces could be energetically and kinetically well differentiated.

Table 3 shows the distances between the cation and the center of the pentagonal ring placed at the bottom of the bowl, for

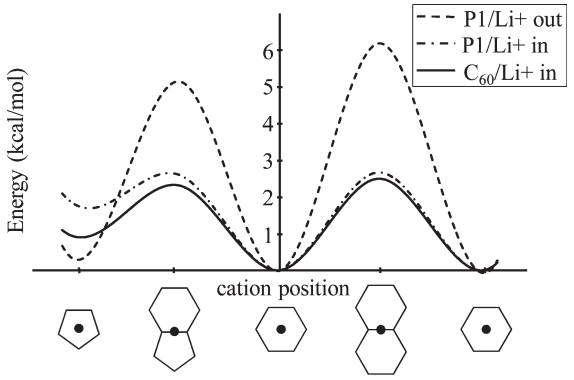

Figure 3. Barriers for face-to-face migration in the system P1/Li^+. For comparison, results of ref 15 for Li^+@C_{60} are included. The full circles in the pictures indicate the positions of the ion (above a ring or C−C bond). In all of the curves the zero value is the energy of the global minima in these systems: complexes with Li^+ centered over one hexagonal face.

complexes with the cation located on the symmetry axis of the MB. In complexes formed with the convex side of all bowls and C_{60} the distances ring-cation are similar to the separation observed in other complexes between π systems (for example benzene) and the same alkaline cation, whereas only Li^+ and Na^+ show a similar behavior for complexes with the inner side. For larger cations (K^+, Rb^+ and Cs^+) inside the MBs a pulling

dx.doi.org/10.1021/jp109654e |J. Phys. Chem. B 2011, 115, 2774–2782

Table 3. Distances (in Ångstroms) from the bottom Plane of the Bowl to the Cations and to the Minima of MEP along the C5 Axis of the Bowls (Figure 1)[a]

	Li^+	Na^+	K^+	Rb^+	Cs^+	MEP min
			inner complexes			
P1 = $C_{20}H_{10}$	1.912	2.418	2.900	3.218	3.504	**2.708**
P2 = $C_{30}H_{10}$	1.923	2.498	3.097	3.482	3.963	**3.726**
P3 = $C_{40}H_{10}$	1.908	2.556	3.442	3.811	4.316	**4.295**
P4 = $C_{50}H_{10}$	1.892	2.516	4.908	4.910	4.919	**5.383**
P5 = $C_{55}H_{10}$	1.870	2.515	2.966	3.327	3.340	**3.630**
C_{60} P face	1.864	2.491	3.332	3.350	3.353	**3.375**
			outer complexes			
P1 = $C_{20}H_{10}$	1.921	2.413	2.906	3.209	3.477	**2.451**
P2 = $C_{30}H_{10}$	1.954	2.423	2.932	3.208	3.475	**2.920**
P3 = $C_{40}H_{10}$	1.942	2.422	2.921	3.231	3.465	**3.340**
P4 = $C_{50}H_{10}$	1.931	2.415	2.911	3.214	3.509	**3.200**
P5 = $C_{55}H_{10}$	1.931	2.416	2.913	3.249	3.504	**3.137**
C_{60} P face	1.933	2.429	2.943	3.249	3.502	
C_6H_6	*1.886*	*2.391*	*2.909*	*3.252*	*3.535*	***1.933***

[a] In the inner complexes of C_{60} with K^+, Rb^+, and Cs^+, the cation is placed in the center of the fullerene structure. Complexes with benzene are included for comparison.

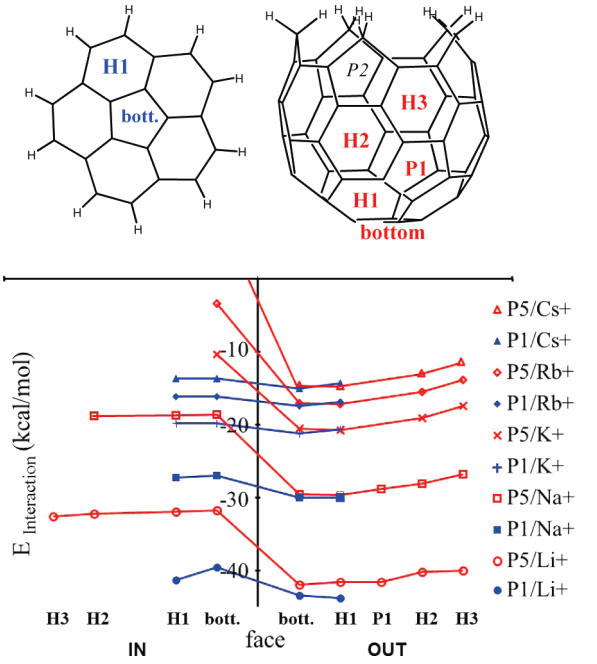

Figure 4. Interaction energies for complexes of alkaline cations with the smallest (P1) and largest (P5) molecular bowls studied.

out of the cation is observed. The distance between the cation and the bottom of the MB increases markedly in the sequence P1−P2−P3−P4. In P5 the walls of the bowl start closing over the cation and repulsion forces move it nearer the bottom. In the inner complexes of C_{60} with K^+, Rb^+, and Cs^+, the cations are located in the center of the fullerene cage, their interaction energy being positive and increasing with cation size (Table 2).

In opposition to the results obtained with cation complexes of other nonplanar π systems,[10e] the geometrical differences observed in the structure of these MBs before and after the formation of the complex are very small. In the case of bowls related with fullerenes, there are systems[3,13, 16] where the formation of the complex causes significant geometrical changes in the structure of the MB, but these results correspond to complexes with transition-metal atoms. The participation of transition metals allows π (MB) → d (metal) donation and d (metal) → π^* (MB) back-donation interactions[12e,17] that are not present in complexes with alkaline cations. In the systems studied in this work, the major changes observed in the MB diameter are in the inner complexes P3/Rb^+ and P4/Cs^+ but both below 0.5% with respect to the diameter of the respective isolated MB. In concordance with these results, deformation energies are about 2% of the interaction energy with the only exception of the inner complexes P4/Cs^+ and P5/Rb^+ (Supporting Information).

Table 2 shows the interaction energies calculated at the computational level described above for all complexes studied in this work. The expected differences between cations are observed, with very intense interaction energies for Li^+ complexes that decrease with the polarizing power of the cation. In all cases, the most stable complex for any MB/cation pair is located in the outer side, as outlined before[12,13] and in agreement with the behavior observed for the MEPs (Figures 1 and 2).

As examples of how the interaction is affected by the cation and bowl nature, the results of two extreme cases, corannulene (P1) and the practically closed P5 are shown in Figure 4. Once again, no significant differences are observed in the outer faces where the trends are regular and the values similar among the corresponding complexes of P1 and P5, but the inner faces give rise to distinctive behaviors. By increasing the size of the cation the steric hindrance in complexes formed with the concave side of the MBs becomes more intense, especially in the closed structures of P4 and P5. This causes that complexes with K^+, Rb^+ and Cs^+ are manifestly less stable than the corresponding complexes with the outer side of large MBs. The maximum effects are found for P5/Cs^+_in where the interaction is repulsive, as well as in the complexes C_{60}/K^+_in, C_{60}/Rb^+_in, and C_{60}/Cs^+_in.

For each cation, the most relevant stability differences observed in Figure 4 and Table 2 are caused by the in/out MB asymmetry. Nevertheless, it is interesting to rationalize (if possible) the effect of the MB face where the cation complexes. For P1, the most stable Li^+ complex locates the cation in the outer side of the peripheral H1 face (P1H1_out), 0.31 kcal/mol more stable than the bottom_out complex. The following members of the series show the same trend: the Li^+ minimum is located in P2P1_out, P3H2_out, and P4H3_out, all over the rings of the rim of P2, P3, and P4, respectively. P5 breaks this tendency, the most stable being the minimum presenting Li^+ in the bottom_out position, although the adjacent P5H1/Li^+_out and P5P1/Li^+_out are both less than 0.5 kcal/mol apart. The other cations prefer the bottom_out site of P1, but the energy differences are lower than 1 kcal/mol in comparison with the interaction energy in P1H1_out. For P2 and P3, the large cations choose the outer faces: P2H1_out and P3H2_out, but in P4 and P5 the H1_out position is preferred by Na^+, K^+, Rb^+, and Cs^+, always with minor differences (less than or about 0.5 kcal/mol) with respect to the complexes in the bottom_out position. At first sight, an explanation that includes all of the tendencies observed does not become apparent.

The influence of the MB size depends on the face and the side of the MB where the complex is formed. As the only two faces common to all the series are the bottom and H1 faces, the

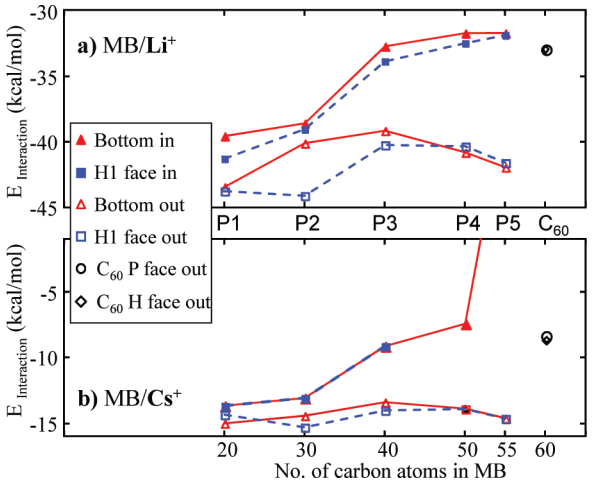

Figure 5. Interaction energies for complexes formed by Li^+ (a) and Cs^+ (b) with the molecular bowls by its bottom and H1 faces.

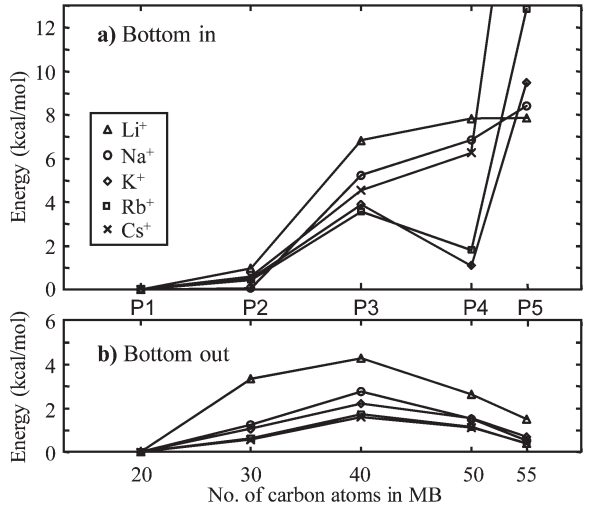

Figure 6. Interaction energies relative to the interaction between P1 and each cation: ΔE interact. $_{Pi/Cat} = E$ interact. $_{Pi/Cat} - E$ interact. $_{P1/Cat}$.

complete examination can be done only using the complexes formed on these sites (Figure 5). With each alkaline cation in the bottom position, the most stable complexes are those formed with P1, and the stability regularly decreases as the open MB series grows up to P3: interaction energy (including signs) P1 < P2 < P3. This sequence is almost linear for the outer complexes but more irregular in the inner ones. Beyond this point, the stability of the complexes in the inner side continues decreasing (interaction energy: P3 < P4 < P5) with the exception of complexes of P4 with K^+ and Rb^+. However, the outer side complexes restabilize for the larger bowls (interaction energy: P3 > P4 > P5) again in an almost linear way.

For inner complexes with the H1 face, the interaction energy trend is similar to that observed in bottom_in complexes. In the case of outer complexes with the H1 face, the most stable ones are formed with P2 and the more unstable with P3 and P4, with virtually the same interaction energies. For the five alkaline cations, P1H1 complexes are a little less stable than P2H1 complexes, and P5H1 slightly more stable than P3H1 or P4H1.

The influence of bowl size over the interaction is summarized in Figure 6 using the interaction energies relative to the corresponding value of the P1/cation complexes. It can be appreciated

Table 4. NBO Charges on Cations (Li^+ and Na^+) in Complexes Formed with the MBs in the Bottom Face

	P1	P2	P3	P4	P5
			inner complexes		
Li^+	0.8612	0.8112	0.6411	0.6988	0.6754
Na^+	0.9417	0.8288	0.7359	0.6540	0.5942
			outer complexes		
Li^+	0.9060	0.9092	0.9087	0.9053	0.9020
Na^+	0.9396	0.9591	0.9674	0.9748	0.9556

that in the outer complexes the trends are similar for all the cations: complexes with bigger bowls are always less stable than the complexes with P1 (the relative energy is always positive) but the relative energy increases from P1 to P3 and decreases again from P3 to P5. In the cases of outer complexes in part b of Figure 6, the progression observed in complexation energies roughly resembles that of the electrostatic potential shown in part b of Figure 1, but for inner complexes in part a of Figure 6 the interaction energies do not follow the same trend as shown by MEP.

Considering the electrostatic interactions alone (usually accepted as the predominant contribution in cation−π interactions) the most stable complexes should be formed with the bowls with more negative MEP. Nevertheless, as the conjugation increases the bowls become more polarizable and the inductive effects become more important. The trends in part b of Figure 6 for the outer complexes could be better explained by the balance of these two factors. As the bowl grows, the electrostatic contribution decreases (MEP reduces) but the induction is greater (polarizability increases) and the less attractive combination of both effects is reached in P3. For the largest ions (K^+, Rb^+, and especially Cs^+) inside the closed bowls (P4 and P5) steric effects add to the previous contributions distorting the trends, the interaction being weaker than expected, and even repulsive for Cs^+ inside P5.

When the complexes are formed the bowl transfers some of its (negative) charge to the cation. The amount of charge transferred to the cation has been considered as an important parameter related with the stability of the cation−π complexes.[18] In the systems studied in the present work, the change in cation charge is a minor effect in the outer complexes (Table 4). However, the change in cation charge is more important when the cation is inside the bowl and there is an inverse relationship between the charge transferred to the cation and the stability of the inner complexes. This trend is opposite to the one previously observed in other complexes of cations with linear and cyclic (not curved) π systems.[18]

To obtain more insight on the nature of the interaction, a simplified partition method has been implemented to examine the relative importance of the major contributions to the interaction energy, especially inductive and electrostatic. For this purpose, we have used the results of two complementary electronic calculations. First of all, using the optimized geometry of the complex, the cation is removed and the MEP value is determined in its location, giving the value of the electrostatic contribution ($E_{electrostatic}$). In the other calculation, the cation is substituted by a point charge of magnitude +1 and the energy of the system is calculated again. The difference between this energy and that of the MB gives the electrostatic + inductive contribution (elsewhere[12e] called the "ionic" contribution), which

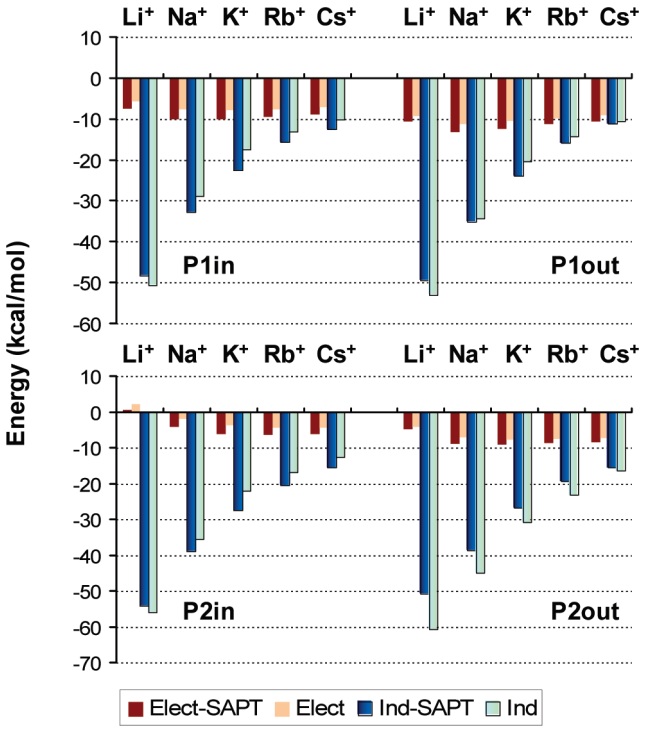

Figure 7. Comparison of electrostatic and induction contributions as obtained with SAPT(DFT) and the simplified partition procedure explained in the text for the complexes of P1 and P2 with the alkaline cations.

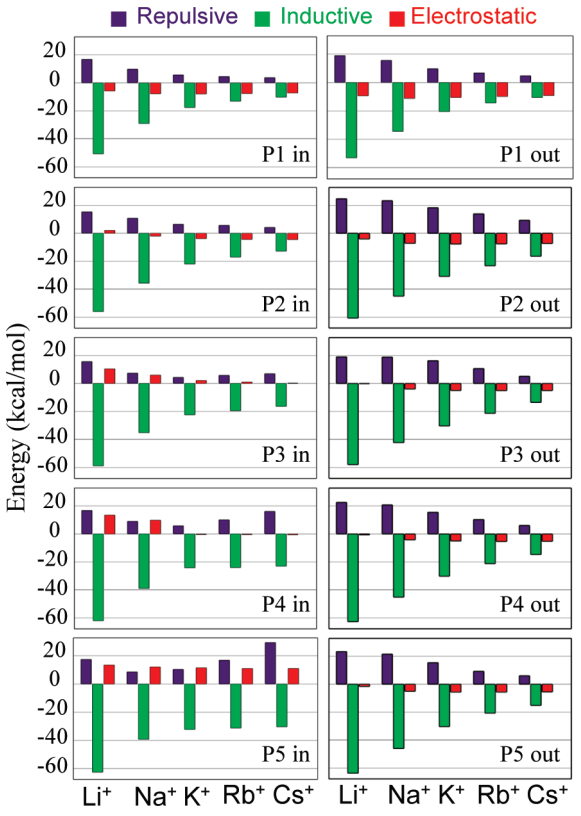

Figure 8. Contributions to the interaction energy (the partition procedure is explained in the text) for the complexes formed by alkaline cations and the bowls studied in the present work.

combined with the previous result allows the calculation of the inductive contribution ($E_{inductive}$). Once these components are substracted from the interaction energy the rest of the contributions are gathered together in a term called here as "Erepulsive". The following equation shows the decomposition done:

$$E_{interaction} = E_{electrostatic} + E_{inductive} + E_{repulsive}$$

Of course, it cannot be expected for this simple model to give a quantitative and rigorous description of the various contributions to the interaction energy, but it can be awaited to describe the main aspects of the interaction for systems controlled mainly by electrostatic−inductive interactions.[12e,19] In any case, the performance of the method was tested against a more rigorous (and more computationally demanding) approach as Symmetry Adapted Perturbation Theory (SAPT) for complexes formed with the two smallest bowls of the series.[20]

Therefore, SAPT(DFT) calculations as implemented in *MOLPRO*[21] were performed at the optimized geometries of the complexes by using the PBEPBE functional with the 6-31+G* basis set (LANL2DZ for Rb and Cs). The asymptotic correction of Grüning was applied with ionization potentials obtained at the same level of calculation,[22] and computational cost was reduced by using density fitting with the def2-TZVP basis sets.[23]

Figure 7 compares the values obtained for the electrostatic and induction contributions as obtained in the simplified partition model with those obtained with the SAPT(DFT) calculations. As expected, both models do not give the same values for the contributions. For example, electrostatic contributions are always less negative in the simplified model, but this can be related with the inability of the model to incorporate penetration effects. In any case, it is worth noting that the simplified partition model is able to reproduce the trends observed in SAPT(DFT) results, even in cases where the calculation predicts a positive electrostatic contribution, as in the complex formed by Li^+ and P2. Also, both methods already show in the smallest bowls how the interaction energy is mainly controlled by induction, whereas the electrostatic contribution is less significant, and even destabilizing. In consequence, though the simplified model is semiquantitative, the results in Figure 7 show that it is powerful enough to represent the most important contributions to the interaction energy and the relative importance of electrostatic and inductive effects. Therefore, and taking into account its modest computational cost, the partition has also been applied to clusters formed with the larger bowls.

Figure 8 shows the results of this simple partition for the complexes with cations located on the symmetry axis of the bowl. As indicated above, the main feature emerging from the partition analysis is that inductive effects prevail over the electrostatic contribution, contrary to the accepted idea that in cation−π complexes the electrostatic interaction dominates. Even when this result agrees with previously reported values obtained with other aromatic− alkaline cation interactions,[24] the semiquantitative level of the model applied here recommends caution and the numerical values should be considered just as a general indication.On the other hand, the relevance of inductive effects explains the already observed dependence of the complexation energy with bowl size.[25]

In the MB/cation complexes, there are many stable complexes with positive electrostatic interaction: all of the inner complexes of P3 and P5 plus P2/Li^+_in, P4/Li^+_in and P4/Na^+_in. All of these complexes are stabilized only by the inductive interaction. The same behavior is expected for all of the fullerene/alkaline

dx.doi.org/10.1021/jp109654e |J. Phys. Chem. B 2011, 115, 2774–2782

cation complexes (as shown in Figure 1, MEP values along the C5 axis of C_{60} are always positive).

A second group of complexes: P3/Li^+_out, P4/Li^+_out and even P5/Li^+_out plus the inner complexes of P4 with K^+, Rb^+, and Cs^+ present a marginal negative electrostatic contribution that cannot explain their stability. In consequence, this group is also mainly stabilized by inductive effects. It can be observed that Li^+ cation is always located much closer to the MB face than the MEP minima (Table 3). So, an important fraction of the electrostatic stabilization energy is lost climbing the electrostatic repulsive wall. This cation, with the highest polarizing power among the alkalines can overcome these losses with the largest inductive effect. In agreement with their lower polarizing power, K^+, Rb^+, and Cs^+ move far away from the bottom of the P4 cavity (with positive MEP) to a position where the MEP value is almost zero, being stabilized by induction.

Finally, in a third group of complexes the cation is located in places where the MEP values are clearly negative. In this case the electrostatic and inductive contributions point in the same direction and these complexes are the most stable ones. This balance between electrostatic and inductive contributions explains the inside−outside selectivity in these MB/cation complexes.

Analyzing the general trends followed by the contributions, it is observed the expected high repulsion at short distances shown mainly for Li^+, but also for Na^+, only exceeded by the repulsion caused by the steric impediment when a big cation is placed inside a closed MB (for example P5/Cs^+_in). The inductive component is clearly dominant in the interaction with high polarizing cations, but less important, though dominant, in complexes with K^+, Rb^+, and Cs^+. This effect is more significant as the polarizability of the MB increases. The electrostatic contribution is roughly determined by the MB's MEP, but the cations are rarely found in the point with the most negative MEP. Small cations move closer to the bowl, hence losing an important amount of electrostatic stabilization (compensated by induction), whereas larger cations are found near the MEP minima or move far away in a region where the MEP-distance dependency has small slopes, leading to electrostatic interactions similar to those predicted by the MB's MEP.

CONCLUSIONS

The interaction of alkaline cations with molecular bowls (MB), curved π systems derived from C_{60}, has been computationally studied by using the B3LYP method with the 6-31+G* (for C, H, Li, Na, and K) and LANL2DZ (for Rb and Cs) basis sets. At this level of calculation, all of the alkaline cations form stable complexes with all MBs, with the cation placed on top of the center of all of the hexagonal and pentagonal rings of the MBs (except in the outermost pentagons of $C_{55}H_{10}$ = P5, the only including saturated carbon atoms). This is true for the interaction with the outer part of the bowls, but the variety of complexes is rather limited for the inner side, due to the curvature and steric impediments. No stable complexes were found with the cation placed on top of atoms or on the edges of the bowls.

The stability of these complexes depends on both the cation and the MB nature, but no general rule applies to all combinations of possible interactions between cations and bowls. Contrary to previous results regarding cation complexes with linear and planar π systems, neither simple numerical relationships between the interaction energy and the distance to the cation, nor with the charge transferred to the cation are found. Instead, a combination of electrostatic and inductive forces governs the interaction energy. The curvature of these π systems generates a concave/convex asymmetry in the electrostatic potential, showing more negative MEP always in their convex (outer) side. In consequence, the more stable complexes are formed with the cation in the outer side of the bowl. The polarizing power of the cation strongly affects the interaction in the expected way: Li^+ and Na^+ (particularly Li^+) are able to compensate part of the loss on electrostatic stabilization by inductive effects, forming complexes at equilibrium distances shorter than the MEP minima. When the MB has a closed structure and the cation is in the concave (inner) side, the repulsive interactions also play an important role in the complexation with larger cations (K^+, Rb^+, and Cs^+).

Finally, the interaction energy has been roughly partitioned into various contributions, such as electrostatic, inductive, and repulsive contributions. Although simple, the partition thus employed allows rationalizing the observed trends. In particular, it emphasizes the importance of the inductive contribution that generally dominates over the electrostatic one in these MB/alkaline cation complexes.

ASSOCIATED CONTENT

Supporting Information. Tables of the contributions to the interaction energies, the deformation energies and the optimized geometries of C_{60}, the MBs and its complexes in the bottom face. This material is available free of charge via the Internet at http://pubs.acs.org.

AUTHOR INFORMATION

Corresponding Author
*E-mail: caba.lago@usc.es.

ACKNOWLEDGMENT

The authors thank the Xunta de Galicia for financial support (project Incite09209103PR and "Axuda para a Consolidación e Estructuración de unidades de investigación competitivas do Sistema Universitario de Galicia, 2007/50, cofinanciada polo FEDER 2007-2013"). The authors want to express their gratitude to the CESGA (Centro de Supercomputación de Galicia) for the use of their computers and to Dr. Yamil Simón-Manso of the National Institute of Standards & Technology (NIST) for its insightful comments offered during the analysis of the manuscript.

REFERENCES

(1) (a) Dougherty, D. A. *Science* **1996**, *271*, 163–168. (b) Ma, J. C.; Dougherty, D. A. *Chem. Rev.* **1997**, *97*, 1303–1324. (c) Meyer, E. A.; Castellano, R. K.; Diederich, F. *Angew. Chem., Int. Ed.* **2003**, *42*, 1210–1250.

(2) (a) Roelens, S.; Torriti, R. *J. Am. Chem. Soc.* **1998**, *120*, 12443–12452. (b) Bartoli, S.; Roelens, S. *J. Am. Chem. Soc.* **1999**, *121*, 11908–11909. (c) Liu, T.; Gu, J. D.; Tan, X. J.; Zhu, W. L.; Luo, X. M.; Jiang, H. L.; Ji, R. Y.; Chen, K. X.; Silman, I.; Sussman, J. L. *J. Phys. Chem. A* **2001**, *105*, 5431–5437. (d) Liu, T.; Gu, J. D.; Tan, X. J.; Zhu, W. L.; Luo, X. M.; Jiang, H. L.; Ji, R. Y.; Chen, K. X.; Silman, I.; Sussman, J. L. *J. Phys. Chem. A* **2002**, *106*, 157–164. (e) Bartoli, S.; Roelens, S. *J. Am. Chem. Soc.* **2002**, *124*, 8307–8315. (f) Cheng, Y. H.; Liu, L.; Fu, Y.; Chen, R.; Li, X. S.; Guo, Q. X. *J. Phys. Chem. A* **2002**, *106*, 11215–11220.

(3) Filatov, A. S.; Petrukhina, M. A. *Coord. Chem. Rev.* **2010**, *254*, 2234–2246.

(4) Frisch, M. J.; Trucks, G. W.; Schlegel, H. B.; Scuseria, G. E.; Robb, M. A.; Cheeseman, J. R.; Montgomery, J. A.; Jr.; Vreven, T.; Kudin, K. N.; Burant, J. C.; Millam, J. M.; Iyengar, S. S.; Tomasi, J.; Barone, V.; Mennucci, B.; Cossi, M.; Scalmani, G.; Rega, N.; Petersson, G. A.; Nakatsuji, H.; Hada, M.; Ehara, M.; Toyota, K.; Fukuda, R.; Hasegawa, J.; Ishida, M.; Nakajima, T.; Honda, Y.; Kitao, O.; Nakai, H.; Klene, M.; Li, X.; Knox, J. E.; Hratchian, H. P.; Cross, J. B.; Adamo, C.; Jaramillo, J.; Gomperts, R.; Stratmann, R. E.; Yazyev, O.; Austin, A. J.; Cammi, R.; Pomelli, C.; Ochterski, J. W.; Ayala, P. Y.; Morokuma, K.; Voth, G. A.; Salvador, P.; Dannenberg, J. J.; Zakrzewski, V. G.; Dapprich, S.; Daniels, A. D.; Strain, M. C.; Farkas, O.; Malick, D. K.; Rabuck, A. D.; Raghavachari, K.; Foresman, J. B.; Ortiz, J. V.; Cui, Q.; Baboul, A. G.; Clifford, S.; Cioslowski, J.; Stefanov, B. B.; Liu, G.; Liashenko, A.; Piskorz, P.; Komaromi, I.; Martin, R. L.; Fox, D. J.; Keith, T.; Al-Laham, M. A.; Peng, C. Y.; Nanayakkara, A.; Challacombe, M.; Gill, P. M. W.; Johnson, B.; Chen, W.; Wong, M. W.; Gonzalez, C.; and Pople, J. A. *Gaussian 03*, Rev. C.01; Gaussian, Inc.: Wallingford CT, 2004.

(5) (a) Becke, A. D. *J. Chem. Phys.* **1993**, *98*, 5648–5652. (b) Lee, C. T.; Yang, W. T.; Parr, R. G. *Phys. Rev. B* **1988**, *37*, 785–788. (c) Miehlich, B.; Savin, A.; Stoll, H.; Preuss, H. *Chem. Phys. Lett.* **1989**, *157*, 200–206.

(6) (a) Hay, P. J.; Wadt, W. R. *J. Chem. Phys.* **1985**, *82*, 270–283. (b) Wadt, W. R.; Hay, P. J. *J. Chem. Phys.* **1985**, *82*, 284–298. (c) Hay, P. J.; Wadt, R. W. *J. Chem. Phys.* **1985**, *82*, 299–316.

(7) (a) Yang, Y.; Weaver, M. N.; Merz, K. M. *Phys. Chem. A* **2009**, *113*, 9843–9851. (b) Li, X. J. *J. Mol. Struct.* **2009**, *896*, 25–29. (c) Rabilloud, F. *J. Phys. Chem. A* **2010**, *114*, 7241–7247. (d) Petrukhina, M. A.; Andreini, K. W.; Mack, J.; Scott, L. T. *J. Org. Chem.* **2005**, *70*, 5713–5716.

(8) (a) Boys, S. B.; Bernardi, F. *Mol. Phys.* **1970**, *19*, 553–566. (b) Chalasinski, G.; Szczesniak, M. M. *Chem. Rev.* **2000**, *100*, 4227–4252.

(9) (a) Haddon, R. C.; Scott, L. T. *Pure Appl. Chem.* **1986**, *58*, 137–142. (b) Haddon, R. C. *J. Am. Chem. Soc.* **1987**, *109*, 1676–1685. (c) Haddon, R. C. *J. Phys. Chem. A* **2001**, *105*, 4164–4165.

(10) (a) Schulman, J. M.; Disch, R. L. *J. Comput. Chem.* **1998**, *19*, 189–194. (b) Priyakumar, U.; Deva; Sastry, G. Narahari *J. Mol. Struct.* **2004**, *674*, 69–75. (c) Dinadayalane, T. C.; Afanasiev, D.; Leszczynski, J. *J. Phys. Chem. A* **2008**, *112*, 7916–7924. (d) Sygula, A.; Saebø, S. *Int. J. Quantum Chem.* **2009**, *109*, 65–72. (e) Bronstein, H. E.; Choi, N.; Scott, L. T. *J. Am. Chem. Soc.* **2002**, *124*, 8870–8875.

(11) Baldridge, K. K.; Siegel, J. S. *Theor. Chem. Acc.* **1997**, *97*, 67–71.

(12) (a) Frash, M. V.; Hopkinson, A. C.; Bohme, D. K. *J. Am. Chem. Soc.* **2001**, *123*, 6687–6695. (b) Priyakumar, U. D.; Sastry, G. N. *Tetrahedron Lett.* **2003**, *44*, 6043–6046. (c) Priyakumar, U. D.; Punnagai, M.; Krishnamohan, G. P.; Sastry, G. N. *Tetrahedron* **2004**, *60*, 3037–3043. (d) Kandalam, A. K.; Rao, B. K.; Jena, P. *J. Phys. Chem. A* **2005**, *109*, 9220–9225. (e) Dunbar, C. *J. Phys. Chem. A* **2002**, *106*, 9809–9819.

(13) (a) Petrukhina, M. A.; Sevryugina, Y.; Rogachev, A. Yu.; Jackson, E. A.; Scott, L. T. *Organometallics* **2006**, *25*, 5492–5495. (b) Seiders, T. J.; Baldridge, K. K.; O'Connor, J. M.; Siegel, J. S. *Chem. Commun* **2004**, *8*, 950–951. (c) Seiders, T. J.; Baldridge, K. K.; O'Connor, J. M.; Siegel, J. S. *J. Am. Chem. Soc.* **1997**, *119*, 4781–4782.

(14) (a) Kamieth, M.; Klärner, F. G.; Diederich, F. *Angew. Chem., Int. Ed.* **1998**, *110*, 3497–3500. (b) Klärner, F. G.; Panitzky, J.; Preda, D.; Scott, L. T. *J. Mol. Model* **2000**, *6*, 318–327. (c) Ansems, R. B. M.; Scott, L. T. *J. Phys. Org. Chem.* **2004**, *17*, 819–823. (d) Scott, L. T.; Bronstein, H. E.; Preda, D. V.; Ansems, R. B. M.; Bratcher, M. S.; Hagen, S. *Pure Appl. Chem.* **1999**, *71*, 209–219.

(15) Bernshtein, V.; Oref, I. *Phys. Rev. A* **2000**, *62*, 033201/1–033201/6.

(16) (a) Amaya, T.; Sakane, H.; Hirao, T. *Angew. Chem.* **2007**, *119*, 8528–8531. (b) Vecchi, P. A.; Alvarez, C. M.; Ellern, A.; Angelici, R. J.; Sygula, A.; Sygula, R.; Rabideau, P. W. *Angew. Chem., Int. Ed.* **2004**, *43*, 4497–4500.

(17) Song-Lin, Z.; Lei, L.; Yao, F.; Qing-Xiang, G. *J. Mol. Struct.* **2005**, *757*, 37–46.

(18) Reddy, A. S.; Sastry, G. N. *J. Phys. Chem. A* **2005**, *109* 8893–8903.

(19) Luque, F. J.; Orozco, M. *J. Comput. Chem.* **1998**, *19*, 866–881.

(20) (a) Jeziorski, B.; Moszynski, R.; Szalewicz, K. *Chem. Rev.* **1994**, *7*, 1887–1930. (b) Misquitta, A. J.; Podeszwa, R.; Jeziorski, B.; Szalewicz, K. *J. Chem. Phys.* **2005**, *123*, 214103/1–214103/14.

(21) Werner H.-J., Knowles P. J., Lindh R., Manby F. R., Schültz M., and others, Molpro version 2009.1, a package of ab initio programs, see http://www.molpro.net (2009).

(22) Grüning, M.; Gritsenko, O. V.; van Gisbergen, S. J. A.; Baerends, E. J. *J. Chem. Phys.* **2001**, *114*, 652.

(23) Weigend, F. *J. Comput. Chem.* **2007**, *29*, 167.

(24) (a) Soteras, I.; Orozco, M.; Luque, F. J. *Phys. Chem. Chem. Phys.* **2008**, *10*, 2616–2624. (b) Kim, D.; Hu, S.; Tarakeshwar, P.; Kim, K. S.; Lisy, J. M. *J. Phys. Chem. A* **2003**, *107*, 1228–1238.

(25) Vijay, D.; Sastry, G. N. *Phys. Chem. Chem. Phys.* **2008**, *10* 582–590.